

Multi-trial Neural Architecture Search with Lottery Tickets

Zimain Wei, Hengyue Pan, Xin niu, Peijie Dong, Dongsheng Li

College of Computer, National University of Defense Technology, Changsha 410073, China

Abstract

In this paper, we propose MENAS, an efficient multi-trial evolution-based NAS method with less human intervention. Specifically, we propose an enlarged search space (MobileNet3-MT) for ImageNet-1K and improve the search efficiency from two aspects. First, MENAS jointly explores architectures and optimal pruned candidates (Lottery Tickets), gradually slimming the average model in populations. Each model is trained with an early stop and replaced by its Lottery Tickets, instead of first searching for a cumbersome network then conducting pruning. Second, we introduce individual weight sharing, which is dedicated to multi-trial NAS, aiming to amortize the training costs by sharing weights between parents and child networks. Compared with weight sharing in supernet, individual weight sharing attains more reliable rank consistency, meanwhile is easy to implement by preventing the sophisticated supernet training. Moreover, to regularize the evolutionary process from trapped in small models, we preserve a small ratio of the largest models when formulating parent populations, which is proved beneficial to enhance model performance. Extensive experiment results demonstrate the superiority of MENAS. On ImageNet-1K database, MENAS achieves 80.5% top-1 accuracy without involving knowledge distillation or larger image resolution. Code and models will be available.

Introduction

The significant success of deep learning in many tasks, like image classification and object detection, is mainly due to the outstanding neural network architectures. Along with this success, many researchers have delivered efforts in designing excellent neural networks, i.e. ResNet [15], MobileNet [28], ConvNext [22] and etc. However, manual designing a powerful architecture is tedious and requires a lot of human endeavors. Neural architecture search (NAS), which is emerged to automate the neural architecture design process, has drawn growing interest.

Different solutions to tackle the NAS problem have been explored in the past few years, as mentioned in [8], they can be coarsely divided into two categories: multi-trial NAS [26, 11, 35], and weight-sharing NAS [2, 21, 37, 3]. Multi-trial NAS performs independent training for different networks. Existing multi-trial NAS works explore the search space by evolutionary [26] or reinforcement algorithm [30], then train each network from scratch. Most of these methods

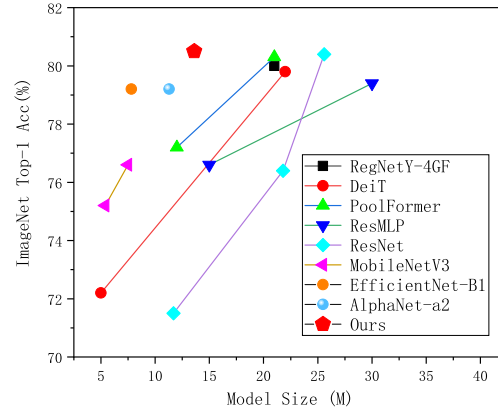


Figure 1: Comparing ImageNet-1K results with other state-of-the-art models of similar model sizes.

suffer from high computation costs. Weight-sharing NAS trains an over-parameterized supernet, and select potential sub-net by sharing weights from the supernet [2, 14, 41, 5] or continuous relaxation [21, 37, 40]. Although they have shown appealing efficiency, weight-sharing NAS methods intrinsically exist several problems. The first one is that their search spaces are highly restricted, in order to constrain the supernet for fast convergence [14, 3], and accommodate all sub-nets on homogeneous building blocks [5, 2]. Limited search space may hinder their practical applications and lead to sub-optimal results due to the human thinking paradigm. Another problem is that the training process for supernet is sophisticated. [2] proposed a gradually shrinking training procedure to train a once-for-all supernet. With multiple stages and carefully designed hyper-parameters, the total training cost takes 12000 hours on 32 GPUs, which is computation prohibitive. Finally, as mentioned by [8, 6], the rank orders of sub-networks that are extracted from the supernet and individually trained are less correlated. This issue tends to be more severe when the search space gets larger. In contrast, multi-trial NAS enjoys more reliable rank consistency, flexible application scenarios, and can be applied to substantially

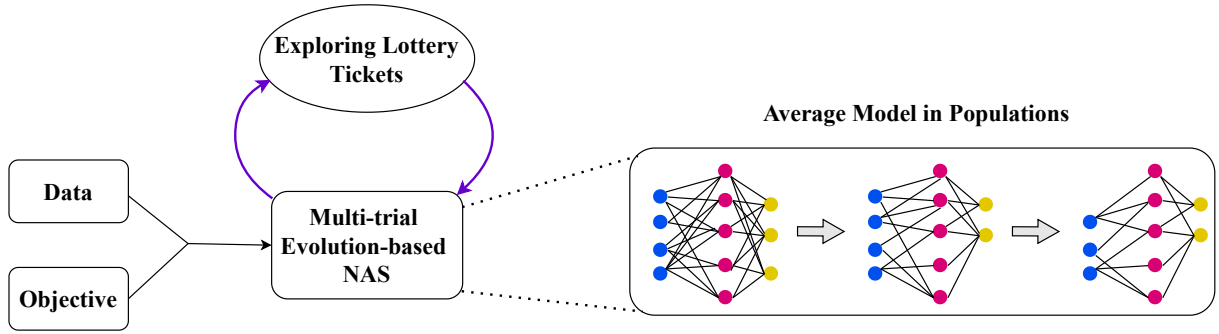


Figure 2: Illustration of searching with Lottery Tickets in MENAS. During the search process, we train each network with an early stop and automatically explore its Lottery Tickets (optimal pruned networks) with minor costs. Then best-performing Lottery Tickets from different networks are utilized to generate child networks for the next generation, gradually slimming the average model in populations.

larger search spaces for better performance. However, multi-trial NAS is less investigated by recent literature due to the high computation cost.

In this paper, we unveil the potential of multi-trial NAS to search in a more challenging search space, where less human intervention is included. Specifically, we propose MENAS, which is a Multi-trial Evolution-based NAS method conducted on an enlarged search space (MobileNet3-MT) for higher performance. Meanwhile, we improve the search efficiency of MENAS from the following two aspects: 1) Gradually slimming the average model in populations to accelerate the search process. 2) Preventing repeated training by individual weight sharing.

For the first aspect, we draw inspirations from structure pruning works[23, 20, 24], which provide substantial speedup by removing model sub-structures, e.g., channels. Specifically, we explore optimal sparse networks within each trained network, which are dubbed as Lottery Tickets [13], promising to achieve the same accuracy with smaller model sizes. The advantages of exploring Lottery Tickets during the search process are two folds: 1) Manual design for efficient networks is prevented since the pruning process automatically generates promising Lottery Tickets. 2) Population is formulated based on excellent smaller networks, gradually reducing the average model size in populations, which in turn accelerates the search process since slimmed networks enjoy faster training speed. Additionally, the cost of exploring Lottery Tickets is minor since back-propagation is not included.

For the second aspect, we introduce individual weight sharing tailored for multi-trial NAS, to essentially reduce the search computation cost. Existing multi-trial NAS methods [30, 26, 42] train each network from scratch, which is computation prohibitive and unnecessary. Weight sharing NAS methods [14, 2, 5] share weights in a sophisticated supernet, with search space restricted and unreliable rank consistency. MENAS absorbs the advantages of multi-trial NAS and weight-sharing NAS, sharing weights as much as possible between parent and child networks since only several architecture operations are changed. It is easy to implement when compared with sophisticated supernet training.

Moreover, to avoid the evolutionary process from being trapped in small models, we propose large model regularization, which keeps a small ratio of the largest models when formulating parent populations. Large models generally attain better accuracy but need more epochs to optimize their parameters. On one hand, the performance of large models may be underestimated when an early stop is conducted during the search process. On the other hand, large models are cumbersome and favorable for discovering Lottery Tickets from a broader range. To this end, we preserve some large models to promote exploring excellent Lottery Tickets, achieving a good trade-off between accuracy and computation.

Extensive experiments demonstrate the effectiveness of MENAS. As presented in Fig. 1, MENAS attains 80.5% top-1 accuracy with 13.6 M parameters, achieving a good trade-off among existing state-of-the-art models. By the proposed accelerating strategies, the search process for MENAS takes 4.8 days on 8 A100 GPUs, which is significantly more efficient than other multi-trial NAS methods. Generally, the contributions of our proposed method are as follows:

- We propose a multi-trial evolution-based NAS framework with an enlarged search space, in which less prior knowledge is included.
- We accelerate the search process by exploring Lottery Tickets and individual weight sharing. Exploring Lottery Tickets gradually reduces the average model in populations, while individual weight sharing prevents repeated training in multi-trial NAS.
- We propose large model regularization to enhance model performance when jointly searching with Lottery Tickets.
- Extensive experiments on ImageNet-1K, CIFAR-10, and CIFAR-100 demonstrate that MENAS achieves state-of-the-art performance.

Approach

We first present the search space we conduct experiments on, following with the overview of the searching process, then we elaborate details of each component in the search process.

Table 1: Comparison of searchable components in different search spaces. MobileNet3-WS (weight sharing) is a restricted sub-search space of MobileNet3-MT (multi-trial). The maximum down-sample number in MobileNet3-MT is fixed as 4. {} represents searchable choices, while (0.7, 0.975, 0.025) means the smallest, the largest, and value intervals. '-' denotes not included.

Component		MobileNet3-WS	MobileNet3-MT (Ours)
Layers	Kernel Size	{3,5,7}	{3,5,7}
	Exapand Rate	{3,6}	{1,2,3,4,5,6}
	SE	✓	{✗, ✓}
Stages	Pruning Rates	-	(0.7, 0.975, 0.025)
	Depth	4	{1,2,3,4,5,6}
	Width Multiplier	-	{ $\frac{1}{2}$, $\frac{5}{8}$, $\frac{3}{4}$, 1, $\frac{5}{4}$, $\frac{3}{2}$, 2}
Downsample		✓, ✓, ✓, ✗, ✓	{{{✗, ✓}}, {{✗, ✓}}, {{✗, ✓}}, {{✗, ✓}}, {{✗, ✓}}}

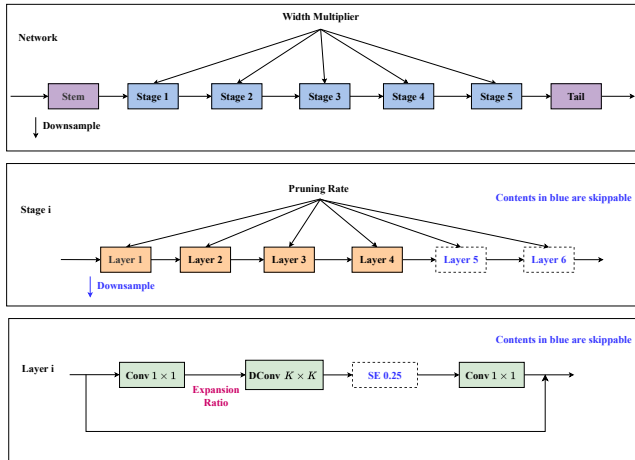


Figure 3: The framework of candidate networks in MobileNet3-MT search space. Similar to [1], each candidate network is grouped into five stages based on output channels. Each stage contains a variable number of layers where only the first layer has stride 2 if a down-sample is conducted. The searchable components for each stage include down-samples, width multipliers, and the number of layers; while that for each layer consists of kernel sizes, expansion ratios, Squeeze-and-Excite modules [18], and the pruning rates. Note that width multipliers are conducted on numbers of output channels for different stages, and pruning rates are used for expansion ratios in inverted bottleneck layers.

Search Space

Our search space is based on MobileNetV3 [17] but attains a much larger cardinality. We present our enlarged search space in Table 1 and show the framework of candidate networks in Fig. 3. For the overall structure of networks, the stem and tail are common, while five stages are searchable. Each stage comprises multiple layers, and each layer is an inverted residual bottleneck. Comparing with search space for weight sharing NAS (e.g., MobileNetV3-WS in Table 1), our MobileNetV3-MT differs in following aspects. First, choices for expansion ratios are extended from {3, 6} to {1,

2, 3, 4, 5, 6}, while depth choices in each stage are enlarged from {2, 3, 4} to {1, 2, 3, 4, 5, 6}. Second, each inverted bottleneck is optionally attached with a Squeeze-and-Excite module (SE) [18]. Down-sampling is also selective for 5 stages with a maximum number of 4 (The first down-sample is conducted in the stem structure). Finally, we search for the width multiplier of each stage and pruning rate to determine the expansion ratio in each inverted bottleneck layer. By enlarging the search space, less human intervention is included, which is favorable to discover more excellent networks.

Overview

To unveil the potential of multi-trial NAS and search in the enlarged challenging search space, the general process of MENAS is as follows:

1. Initialize a population by randomly sampling 60 architectures in the search space.
2. Each network in the population is trained with an early stop (30 epochs) to obtain its search accuracy. For each trained network:
 - (a) Generate 40 pruning proposals. Each proposal represents a non-uniform pruning strategy and derives a new architecture with reduced computation complexity.
 - (b) Initialize the newly pruned architecture by pre-trained weights. Specifically, weights in the origin network will be copied for unchanged layers and truncated from the low index for slimmed layers.
 - (c) Re-calibrate the BN statistics by forward-propagating training data for a few iterations. In this process, the trainable parameters are fixed.
 - (d) Rank newly pruned architectures by inference accuracy and select the top-2 candidate as the Lottery Tickets [13] of the unpruned network.
 - (e) Fine-tune the selected Lottery Tickets for 3 epochs and obtain their search accuracy.
3. Formulate the parent population of size 30 by 80% best-performing Lottery Tickets and 20% the largest models.
4. Mutation and crossover are conducted on the parent population to derive 30 child networks. With individual weight sharing, the training epochs of child networks for the next generations are reduced to 20.

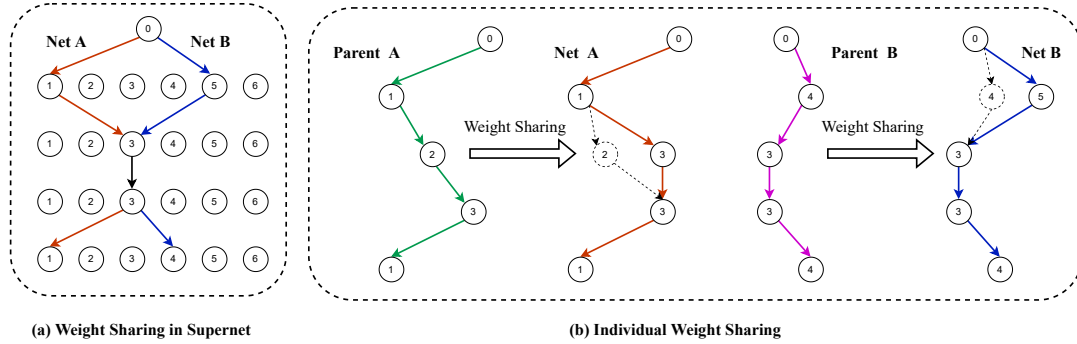


Figure 4: Comparison between weight sharing in supernet (a) and individual weight sharing (b). Numbers 1 ~ 6 refer to different architecture operation choices for each layer. In (a), we take SPOS [14] as an example, when updating Net A, the weights in Net B are affected (we omit other sub-nets for simplicity), leading to slow convergence of the supernet. When the search space is large, weight sharing is conducted among vastly different sub-networks. As a result, the rank consistency between performances of Net A and B inherited from the supernet, and true performances of training independently from scratch, are not guaranteed. In (b), individual weight sharing is conducted, where parent and child networks share weight as much as possible. Individual weight sharing is easy to implement and attains a more reliable performance rank due to independent training.

5. Repeat step 2 ~ 4 for the newly generated population until the end.

Note that the hyper-parameters in the search process are not fixed and can be exchanged based on computation resources. With more carefully tuned hyper-parameters, improved performance can be obtained. We set the fine-tune epoch as 3 since we found from experiments that Lottery Tickets can quickly regain search accuracy in less than 5 epochs. In the following section, we will present details of exploring Lottery Tickets, individual weight sharing, and large model regularization.

Exploring Lottery Tickets

Background Lottery Ticket is proposed by [13], which refers to sparse sub-networks contained in standard dense networks capable of training in isolation to match the test accuracy of the original network. Follow-up work [39] further shows that Lottery Ticket can be identified at an early training stage, instead of requiring the costly full training process. To this end, exploring Lottery Ticket can be naturally incorporated into our search process where an early stop is conducted.

Our paradigm Instead of first searching for a cumbersome network, then conducting pruning to obtain its Lottery Ticket, we directly adopt exploring Lottery Ticket as a fine-grained search level. As depicted in Fig. 2, exploring Lottery Ticket and neural architecture search are conducted simultaneously. The exploration of Lottery Tickets is efficient and automatic. We present details in the following two steps: 1) initialization, 2) BN calibration and inference.

Initialization The pruning proposal of each trained network is denoted as (p_1, p_2, \dots, p_i) , where p_i is the pruning rate of the i -th layer. Generally, there are three scenarios for the weight shape of the i -th layer in the unpruned network: (1) For convolution layers, the weight is a four-dimension tensor with shape (C_{out}, C_{in}, K, K) . K is the kernel size of the

convolution layer. (2) For fully connected layers, the weight is a two-dimension tensor with shape (C_{out}, C_{in}) . (3) For BatchNorm layers, the weight shape is (C_{out}) . Therefore, the weight matrix W^* of the pruned layer is obtained as follows:

$$W^* = \begin{cases} W[:, C_{out} \times p_i, :, C_{in} \times p_{i-1}, :, :] & W \in \mathbb{R}^{(C_{out}, C_{in}, K, K)} \\ W[:, C_{out} \times p_i, :, C_{in} \times p_{i-1}] & W \in \mathbb{R}^{(C_{out}, C_{in})} \\ W[:, C_{out} \times p_i] & W \in \mathbb{R}^{C_{out}} \end{cases} \quad (1)$$

where p_{i-1} is the pruning rate of the $(i-1)$ -th layer, C_{out} and C_{in} are numbers of output and input channels for the i -th layer, respectively.

BN calibration and inference As possible combinations of pruning rates are enormous, we need to spot the best pruning proposals (Lottery Tickets) before actually fine-tuning them. An intuitive methodology is to rank their inference accuracy. Unfortunately, we found empirically that networks generated by pruning proposals show poor and similar accuracy when directly evaluated on the validation data. As mentioned in [20], the reason may lie in the outdated global BN statistics that are copied from unpruned networks. Therefore, we forward-propagate a few iterations on training data to re-calibrate the statistics in batch normalization. Note that when we update the statistics of batch normalization, the trainable parameters of pruned networks are fixed. In this way, we can fast evaluate the potential of pruned networks by inference accuracy and select superior ones as Lottery Tickets to guarantee good performance.

Individual Weight Sharing

Individual weight sharing is conducted between parent and child networks in the evolutionary process. Previously, many state-of-the-art weight-sharing methods tend to share weights within a deeply entangled supernet. As a representative work, Single Path One-Shot (SPOS) [14] accommodates all subnets as different paths in the supernet, then train the supernet

Table 2: Comparison with manual, model-scaling, and automated methods on ImageNet-1K. ‘-’ denotes not available, while ‘N/A’ means not provided by the origin paper. The time costs for [14, 21, 2] include supernet training time and search time. The time cost for MENAS includes both model training time and Lottery Tickets searching time. Models marked with \dagger are trained with knowledge distillation [16].

Architecture	Type	FLOPs	Param	Top-1 Acc.	Time Cost
ResNet-50 [34]	manual	4.1	25.6	79.8	-
EfficientNet-B2 [31]	model scaling	1.0	9.2	80.1	-
RegNet Y-1.6G [25]	auto	1.6	11.2	78.0	N/A
GPUNet-0 [33]	auto	3.3	11.9	78.9	N/A
DenseNAS-R3 [12]	auto	3.4	24.7	78.0	N/A
RandWire-WS, C=109 [36]	auto	4.0	31.9	79.0	N/A
DARTS [21]	auto	0.6	4.7	73.1	5
SPOS [14]	auto	0.3	3.4	74.7	13
MnasNet-A3 [30]	auto	0.4	5.2	76.7	288
OnceForAll [2] \dagger	auto	0.6	9.1	80.0	1600
MENAS	auto	1.5	13.6	80.5	38.4
MENAS \dagger	auto	1.5	13.6	81.5	38.4

Table 3: Transfer learning results on downstream classification datasets CIFAR-10 and CIFAR-100. Since label classes have changed, the model parameter is reduced to 12.5 M.

Model	Param	CIFAR-10	CIFAR-100
ViT-B/16 [9]	87M	98.1	87.1
NASNet-A [10]	85M	98.0	87.5
ResNet50-A1 [34]	25.6 M	98.3	86.9
ResMLP-S12 [32]	15.4M	98.1	87.0
DARTS [21]	3.3M	97.2	-
MENAS	12.5M	98.5	88.3

by updating a random path in each iteration. In MENAS, individual weight sharing is performed discretely between parent and child networks. The child networks copy weights of overlapped layers from their trained parents, while randomly initializing newly generated layers. We show their differences in Fig. 4.

In a supernet, weight sharing is conducted among vastly different sub-nets, leading to less rank consistency when the search space is large. Moreover, the supernet training is also challenging. Comparatively, in individual weight sharing, parents are viewed as different small-scaled supernets, sharing weights only with their closest counterparts (child networks). In practice, the path strings that save the checkpoints of each network and its parent are recorded by a dictionary. When a child network starts to be trained, the weights from its parent are loaded based on the path string. With individual weight sharing, the search process is accelerated by avoiding training each network from scratch, and rank consistency is ensured by the multi-trial training paradigm.

Large Model Regularization

In the early model training stage, smaller networks tend to show higher performance than larger counterparts, which may lead to the small model trap [38], where potential larger models may be discarded with slower accuracy increasing speed. To provide a regularization, we preserve a small ratio of large models when formulating parent networks for the next generation. Specifically, we select 80% top-performing Lottery Tickets and 20% models with the largest model size for parent populations. Large model regularization is beneficial to explore well-performed Lottery Tickets from a broader range, achieving a good trade-off between performance and computation cost.

Experiments

We report image classification results on ImageNet-1K [27] and transfer learning results on CIFAR-10, CIFAR-100 to demonstrate the effectiveness of MENAS. Various ablation studies are also presented to shed light on the effects of design decisions.

Experimental Details

For the search process, we randomly sample 10% data of each class from the original 1K-class ImageNet-1K training set for training, while using the same validation set for validation. We set the computation budget (FLOPs) for the search process as $1 \sim 1.6$ G. The population is initialized by randomly sampling 60 networks within the computation budget. Training epochs for the initial population are 30, then reduced to 20 in the following generations since individual weight sharing is conducted. We train our models on 8 GPUs using the RMSProp optimizer with 0.9 momentum, a total batch size of 1024. The learning rate is first warmed up from 0 to

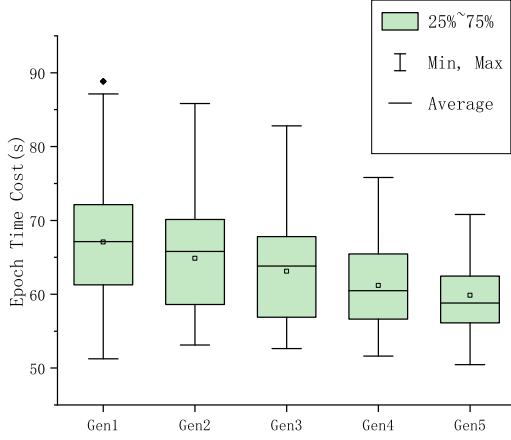


Figure 5: Distribution of time cost per epoch for networks in each generation. The maximum-smallest range and average line are presented. Time cost for each epoch includes training time, validation time, and data loading time in the search process.

0.064, then decayed by 0.97 every 2.4 epochs. The dropout rate applied to the last layer is 0.2. For each model, we generate 40 pruning proposals, from which 2 Lottery Tickets are selected and fine-tuned for 3 epochs. After one generation finishes training, crossover and mutation are conducted on selected parent networks to generate child populations. The total search cost for 5 generations takes 4.8 days on 8 Tesla A100. We present details of the final architecture in supplemental materials. When retraining on the full ImageNet-1K dataset, we use the exponential moving average with 0.9999 decay rate, and RandAugment [7]. The final architecture is trained from scratch with image size 224×224 for 300 epochs.

Results on ImageNet-1K

Table 2 presents the comparison of MENAS with other state-of-the-art models. Without any bells and whistles, MENAS achieves 80.5% top-1 accuracy, surpassing EfficientNet-B2 [31] by 0.4%. When comparing with other NAS methods, MENAS shows a boost of 0.5% top-1 accuracy on OnceForAll [2] while requiring significantly less search cost. Notably, when trained with knowledge distillation [16], MENAS further achieves 81.5% top-1 accuracy, which demonstrates the strong capacity of our method.

Transfer Learning Results

We transfer MENAS to commonly used image recognition datasets CIFAR-10, and CIFAR-100 [19]. ImageNet pre-trained checkpoint is applied and fine-tuned on new datasets. Training hyper-parameters are presented in supplemental materials. Table 3 shows the results of top-1 accuracy for transfer learning. In general, our method consistently reports better accuracy than other state-of-the-art models, suggesting good generality of MENAS.

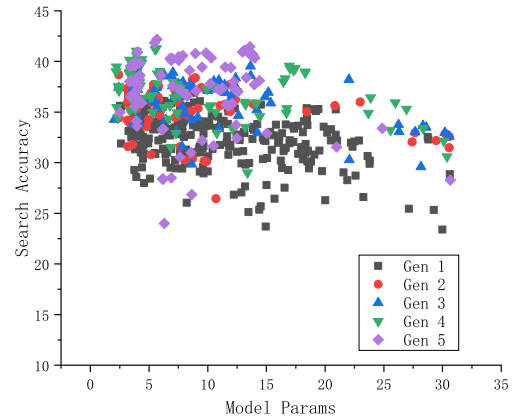


Figure 6: Model parameters vs. search accuracy in 5 generations.

Ablation Studies and Analyses

Effectiveness of Exploring Lottery Tickets To validate the effectiveness of exploring Lottery Tickets in MENAS, we present epoch time cost distribution in Fig .5 and model size distribution in Fig . 6. Epoch time represents the training speed of networks, which is much related to model parameters and computations. It can be observed from Fig .5 that due to the substantial speedup provided by pruning, the average epoch time cost is gradually reduced. Fig . 6 further indicates that the evolutionary process is guided to more efficient and well-performed networks by generations. Moreover, we retrain a randomly sampled architecture and its two Lottery Tickets under the same setting to compare their performance. The training curves are depicted in Fig . 7. It is evident that Lottery Tickets show comparable performance with reduced model sizes, supporting our motivations.

Individual Weight Sharing vs SPOS Weight Sharing To compare the rank consistency of the proposed individual weight sharing and SPOS weight sharing[14], we perform both methods on MobileNet3-WS search space (see Table 1 left for more details). Due to our computation limitation, we conduct those experiments on CIFAR-10. Since the pruning process is orthogonal, we exclude it here for simplicity. In the individual weight sharing setting, we initialize a population by randomly sampling 100 networks and train them for 40 epochs. Best-performing networks are selected as parents to generate our target generation, in which individual weight sharing is conducted and each network is only trained for 25 epochs. To achieve a comparable time cost, we perform model training in parallel on 8 GPUs with one GPU per network during the individual weight sharing setting. In the SPOS weight sharing setting, we build a supernet with each path representing one sub-network. During the 600-epoch supernet training, one random path is updated by one iteration

Table 4: Comparison with random baseline. We measure different search methods with coarsely identical search time. Evaluated networks (N) refer to the number of trained networks in the search process. Gd represents GPU days. For MENAS, the evaluated networks include normally trained networks and fine-tuned Lottery Tickets. All search processes are conducted on a 10% subset of ImageNet and results are obtained by re-training the searched network on the full dataset.

Method	Evaluated Networks	Search Cost	Params	Top-1 Acc.
Random Search	N=200	38.5 Gd	16.9 ± 3.0 M	78.2 ± 0.5
Ours	N=540	38.4 Gd	13.6 M	80.5

Table 5: Comparison of rank consistency under individual weight sharing and SPOS weight sharing settings. Both settings are conducted on MobileNet3-WS search space with the sampled number of networks varies as 10, 20, and 30. Three metrics including RMSE, Spearman, and Kendalls Tau are reported to measure rank consistency between search accuracy and retrain accuracy. For RMSE, a smaller value is better, while Spearman and Kendalls Tau are the opposite. We conduct this experiment on the CIFAR-10 database.

Rank Consistency	SPOS WS			Individual WS		
	10	20	30	10	20	30
RMSE	2.84	2.70	2.78	1.65	1.65	1.64
Spearman	0.20	0.20	0.32	0.32	0.41	0.54
Kendalls Tau	0.09	0.12	0.23	0.24	0.29	0.41

following SPOS [14]. Finally, we sample the same networks from the target generation and the well-trained supernet to obtain their search accuracy in different settings. Each sampled network is also trained from scratch for 600 epochs to obtain its re-train accuracy. RMSE [4], Spearman rank correlation, and Kendalls Tau [29] are applied to measure the rank consistency between the search accuracy and 600-epoch re-train accuracy. Results are summarized in Table 5. It is evident that when the sampled number of networks varies from 10, 20, and 30, individual weight sharing consistently outperforms SPOS weight sharing among all three metrics.

Comparison with Random Search We compare MENAS with the random baseline of coarsely identical search time. Each search process is conducted on a 10% subset of ImageNet-1K, then the selected network is re-trained on the full dataset. The model computation constraint (1~1.6 G FLOPs) for random baseline is the same as MENAS. During the random search, each model is trained for 30 epochs. Results are presented in Table 4. It can be observed that MENAS outperforms the random baseline with smaller model size, indicating the superior of our method.

Large Model Regularization We ablate large model regularization to examine its effectiveness in MENAS. Results are summarized in Table 6. Generally, MENAS without large model regularization achieves an inferior performance. We speculate that it is due to the limited range of exploring Lottery Tickets, leading the evolutionary process biased to smaller models. Therefore, the large model regularization

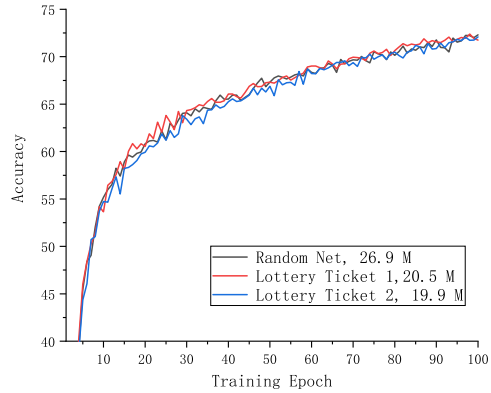


Figure 7: 100-epoch retraining curve on the full ImageNet-1K for a random model and its two Lottery Tickets.

Table 6: Ablation study of large model regularization.

Large Model Regularization	Params	Top-1 Acc.
✗	10.4 ± 3.0 M	78.4 ± 0.2
✓	13.6 M	80.5

is nontrivial to get rid of the small model trap, which helps to discover more potential efficient networks and enhance performance.

Conclusion

In this paper, we propose MENAS, a multi-trial NAS framework with an enlarged search space for higher performance. MENAS tackle the heavy computation problem in exiting multi-trial NAS methods by exploring Lottery Tickets and individual weight sharing. Exploring Lottery Tickets gradually reduces the average model size in populations, which provides substantial speedup for training. Individual weight sharing combines the merits of weight sharing NAS and multi-trial NAS while attaining a more reliable rank consistency. Moreover, large model regularization is proposed to avoid the small model trap in our search process. State-of-the-art performance on ImageNet-1K, CIFAR-10, and CIFAR-100 demonstrate the effectiveness of MENAS.

References

- [1] Bender, G.; Liu, H.; Chen, B.; Chu, G.; Cheng, S.; Kindermans, P.-J.; and Le, Q. V. 2020. Can weight sharing outperform random architecture search? an investigation with tunas. In *Proceedings of the IEEE/CVF Conference on Computer Vision and Pattern Recognition*, 14323–14332.
- [2] Cai, H.; Gan, C.; Wang, T.; Zhang, Z.; and Han, S. 2019. Once-for-all: Train one network and specialize it for efficient deployment. *arXiv preprint arXiv:1908.09791*.
- [3] Cai, H.; Zhu, L.; and Han, S. 2018. Proxylessnas: Direct neural architecture search on target task and hardware. *arXiv preprint arXiv:1812.00332*.
- [4] Chai, T.; and Draxler, R. R. 2014. Root mean square error (RMSE) or mean absolute error (MAE)?—Arguments against avoiding RMSE in the literature. *Geoscientific model development*, 7(3): 1247–1250.
- [5] Chen, M.; Peng, H.; Fu, J.; and Ling, H. 2021. Autoformer: Searching transformers for visual recognition. In *Proceedings of the IEEE/CVF International Conference on Computer Vision*, 12270–12280.
- [6] Cho, H.; Shin, J.; and Rhee, W. 2022. B2EA: An Evolutionary Algorithm Assisted by Two Bayesian Optimization Modules for Neural Architecture Search. *arXiv preprint arXiv:2202.03005*.
- [7] Cubuk, E. D.; Zoph, B.; Shlens, J.; and Le, Q. V. 2020. RandAugment: Practical automated data augmentation with a reduced search space. In *Proceedings of the IEEE/CVF Conference on Computer Vision and Pattern Recognition Workshops*, 702–703.
- [8] Dong, X.; Liu, L.; Musial, K.; and Gabrys, B. 2021. Nats-bench: Benchmarking nas algorithms for architecture topology and size. *IEEE transactions on pattern analysis and machine intelligence*.
- [9] Dosovitskiy, A.; Beyer, L.; Kolesnikov, A.; Weissenborn, D.; Zhai, X.; Unterthiner, T.; Dehghani, M.; Minderer, M.; Heigold, G.; Gelly, S.; et al. 2020. An image is worth 16x16 words: Transformers for image recognition at scale. *arXiv preprint arXiv:2010.11929*.
- [10] Enzo; Leiva-Aravena; Eduardo; Leiva; Vasty; Zamorano; Claudia; Rojas; John; and M. 2019. Neural Architecture Search with Reinforcement Learning. *Science of the Total Environment*.
- [11] Falkner, S.; Klein, A.; and Hutter, F. 2018. BOHB: Robust and efficient hyperparameter optimization at scale. In *International Conference on Machine Learning*, 1437–1446. PMLR.
- [12] Fang, J.; Sun, Y.; Zhang, Q.; Li, Y.; Liu, W.; and Wang, X. 2020. Densely connected search space for more flexible neural architecture search. In *Proceedings of the IEEE/CVF conference on computer vision and pattern recognition*, 10628–10637.
- [13] Frankle, J.; and Carbin, M. 2018. The lottery ticket hypothesis: Finding sparse, trainable neural networks. *arXiv preprint arXiv:1803.03635*.
- [14] Guo, Z.; Zhang, X.; Mu, H.; Heng, W.; Liu, Z.; Wei, Y.; and Sun, J. 2020. Single path one-shot neural architecture search with uniform sampling. In *European Conference on Computer Vision*, 544–560. Springer.
- [15] He, K.; Zhang, X.; Ren, S.; and Sun, J. 2016. Deep residual learning for image recognition. In *Proceedings of the IEEE conference on computer vision and pattern recognition*, 770–778.
- [16] Hinton, G.; Vinyals, O.; Dean, J.; et al. 2015. Distilling the knowledge in a neural network. *arXiv preprint arXiv:1503.02531*, 2(7).
- [17] Howard, A.; Sandler, M.; Chu, G.; Chen, L.-C.; Chen, B.; Tan, M.; Wang, W.; Zhu, Y.; Pang, R.; Vasudevan, V.; et al. 2019. Searching for mobilenetv3. In *Proceedings of the IEEE/CVF International Conference on Computer Vision*, 1314–1324.
- [18] Hu, J.; Shen, L.; and Sun, G. 2018. Squeeze-and-excitation networks. In *Proceedings of the IEEE conference on computer vision and pattern recognition*, 7132–7141.
- [19] Krizhevsky, A.; and Hinton, G. 2009. Learning multiple layers of features from tiny images. *Handbook of Systemic Autoimmune Diseases*, 1(4).
- [20] Li, B.; Wu, B.; Su, J.; Wang, G.; and Lin, L. 2020. EagleEye: Fast Sub-net Evaluation for Efficient Neural Network Pruning. *Springer, Cham*.
- [21] Liu, H.; Simonyan, K.; and Yang, Y. 2018. DARTS: Differentiable Architecture Search. In *International Conference on Learning Representations*.
- [22] Liu, Z.; Mao, H.; Wu, C.-Y.; Feichtenhofer, C.; Darrell, T.; and Xie, S. 2022. A ConvNet for the 2020s. *arXiv preprint arXiv:2201.03545*.
- [23] Liu, Z.; Mu, H.; Zhang, X.; Guo, Z.; Yang, X.; Cheng, K.-T.; and Sun, J. 2019. Metapruning: Meta learning for automatic neural network channel pruning. In *Proceedings of the IEEE/CVF International Conference on Computer Vision*, 3296–3305.
- [24] Liu, Z.; Sun, M.; Zhou, T.; Huang, G.; and Darrell, T. 2018. Rethinking the value of network pruning. *arXiv preprint arXiv:1810.05270*.
- [25] Radosavovic, I.; Kosaraju, R. P.; Girshick, R.; He, K.; and Dollár, P. 2020. Designing network design spaces. In *Proceedings of the IEEE/CVF Conference on Computer Vision and Pattern Recognition*, 10428–10436.
- [26] Real, E.; Aggarwal, A.; Huang, Y.; and Le, Q. V. 2019. Regularized evolution for image classifier architecture search. In *AAAI*.
- [27] Russakovsky, O.; Deng, J.; Su, H.; Krause, J.; Satheesh, S.; Ma, S.; Huang, Z.; Karpathy, A.; Khosla, A.; Bernstein, M.; Berg, A. C.; and Fei-Fei, L. 2015. ImageNet Large Scale Visual Recognition Challenge. *International Journal of Computer Vision (IJCV)*, 115(3): 211–252.
- [28] Sandler, M.; Howard, A.; Zhu, M.; Zhmoginov, A.; and Chen, L.-C. 2018. Mobilenetv2: Inverted residuals and linear bottlenecks. In *Proceedings of the IEEE conference on computer vision and pattern recognition*, 4510–4520.
- [29] Sen, P. K. 1968. Estimates of the regression coefficient based on Kendall's tau. *Journal of the American statistical association*, 63(324): 1379–1389.
- [30] Tan, M.; Chen, B.; Pang, R.; Vasudevan, V.; Sandler, M.; Howard, A.; and Le, Q. V. 2019. Mnasnet: Platform-aware neural architecture search for mobile. In *Proceedings of the IEEE/CVF Conference on Computer Vision and Pattern Recognition*, 2820–2828.
- [31] Tan, M.; and Le, Q. 2019. Efficientnet: Rethinking model scaling for convolutional neural networks. In *International conference on machine learning*, 6105–6114. PMLR.
- [32] Touvron, H.; Bojanowski, P.; Caron, M.; Cord, M.; El-Nouby, A.; Grave, E.; Izacard, G.; Joulin, A.; Synnaeve, G.; Verbeek, J.; et al. 2021. Resmlp: Feedforward networks for image classification with data-efficient training. *arXiv preprint arXiv:2105.03404*.

- [33] Wang, L.; Yu, C.; Salian, S.; Kierat, S.; Migacz, S.; and Florea, A. F. 2022. GPUNet: Searching the Deployable Convolution Neural Networks for GPUs. *arXiv preprint arXiv:2205.00841*.
- [34] Wightman, R.; Touvron, H.; and Jégou, H. 2021. Resnet strikes back: An improved training procedure in timm. *arXiv preprint arXiv:2110.00476*.
- [35] Xie, L.; and Yuille, A. 2017. Genetic cnn. In *Proceedings of the IEEE international conference on computer vision*, 1379–1388.
- [36] Xie, S.; Kirillov, A.; Girshick, R.; and He, K. 2019. Exploring randomly wired neural networks for image recognition. In *Proceedings of the IEEE/CVF International Conference on Computer Vision*, 1284–1293.
- [37] Xu, Y.; Xie, L.; Zhang, X.; Chen, X.; Qi, G.-J.; Tian, Q.; and Xiong, H. 2019. Pc-darts: Partial channel connections for memory-efficient differentiable architecture search. *arXiv preprint arXiv:1907.05737*.
- [38] Yang, Z.; Wang, Y.; Chen, X.; Shi, B.; Xu, C.; Xu, C.; Tian, Q.; and Xu, C. 2020. Cars: Continuous evolution for efficient neural architecture search. In *Proceedings of the IEEE/CVF Conference on Computer Vision and Pattern Recognition*, 1829–1838.
- [39] You, H.; Li, C.; Xu, P.; Fu, Y.; Wang, Y.; Chen, X.; Baraniuk, R. G.; Wang, Z.; and Lin, Y. 2019. Drawing early-bird tickets: Towards more efficient training of deep networks. *arXiv preprint arXiv:1909.11957*.
- [40] Zela, A.; Elsken, T.; Saikia, T.; Marrakchi, Y.; Brox, T.; and Hutter, F. 2020. Understanding and Robustifying Differentiable Architecture Search. *ICML*.
- [41] Zhang, X.; Huang, Z.; Wang, N.; Xiang, S.; and Pan, C. 2020. You only search once: Single shot neural architecture search via direct sparse optimization. *IEEE Transactions on Pattern Analysis and Machine Intelligence*, 43(9): 2891–2904.
- [42] Zoph, B.; Vasudevan, V.; Shlens, J.; and Le, Q. V. 2018. Learning transferable architectures for scalable image recognition. In *CVPR*.